CHALLENGES OF MAKING LOW DENSITY FE-MN-AL-C STEELS

[1,2]Jaka BURJA, [1]Barbara ŠETINA BATIČ, [2]Tilen BALAŠKO, [2]Jožef MEDVED

[1]*IMT - Institute of metals and technology, Ljubljana, Slovenia, EU, jaka.burja@imt.si, barbara.setina@imt.si*

[2] *University of Ljubljana, Ljubljana Faculty of Natural Sciences and Engineering, Slovenia, EU, tilen.balasko@ntf.uni.lj.si, jozef.medved@ntf.uni.lj.si*

https://doi.org/10.37904/metal.2022.4408

Abstract

The topic of low density steels, also called light weight steels, has gained new interest in the last decade. These steels have remarkably low densities around 6.7 kg/l. They are based on the Fe-Mn-Al-C alloy system and contain around 15% Mn and around 10% Al, with high contents of C, around 0.8%. Due to high amounts of alloying elements, their microstructures can be ferritic, austenitic to duplex (also sometimes triplex). Besides the low density, the tensile tests can show elongations up to 90% and strengths above 1000 MPa. The promising steel properties are, however, accompanied by a complicated microstructural evolution, with kappa carbide precipitation and ordering of ferrite. The solidification intervals are about 100 °C, and the slow cooling leads to B2 ordered phase precipitation, and the formation of different morphologies of kappa carbides, that cause embrittlement. Fast cooling prevents secondary precipitation, and avoids phase transformations but the internal and thermal stresses cause cracking. The melting itself is not trivial due to the complex chemistries. The solidification, microstructural evolution and practical cases of heat treatments and hot working, with examples of material failure are monitored.

Keywords: Lightweight steel, low density, annealing, microstructure, microscopy

1. INTRODUCTION

About 20% of EU greenhouse gas emissions comes from the transportation sector, 72% of which comes from road transport [1,2]. That is why car weight reduction directly affects CO_2 emission. Low-density Fe-Mn-Al-C steels show potential, as combine low density with excellent strength and ductility [3-7]. In fact the Steel strength ductility diagram also known as the “Banana diagram” that has been is the subject of numerous scientific and technical publications clearly shows the advantage of this type of steels. It shows a picture of both commercially available, as well as emerging steel grades, with the Fe-Mn-Al-C marked with yellow (**Figure 1**). Essentially it classifies automotive steels, in a metallurgical designation providing some process information. The gray bubbles include lower-strength interstitial-free steels (IF) conventional high strength steels, such as bake hardenable (BH) and high-strength low-alloy steels (HSLA); and Advanced High-Strength Steels (AHSS) such as dual phase and transformation-induced plasticity steels. Additional higher strength steels (green bubble) include steels with special thermomechanical treatment and alloying, these steels are designed for unique applications that have improved edge stretch and stretch bending characteristics, dual phase steels (DP) and complex phase steels (CP) that include intercritical annealing and/or rolling in the two phase zone, martensitic steel with special alloying elements like B, Cr, Ni, Mn, Mo, Si etc. and highly alloyed steels that require unique heat treatments like maraging steel. The high Mn twinning induced plasticity (TWIP) and transformation induced plasticity (TRIP) present another group of steels, where the high Mn content alongside special thermomechanical treatments enable amazing ductility at high strengths (cyan bubble). Besides the obvious advantage in the strength ductility combination, the Fe-Mn-Al-C steels also show low density. Addition of aluminum is an efficient way to reduce the steel mass (1.3% density reduction per 1 wt% Al) [3,8]. These low-density Fe-Mn-Al-C steels have three types of microstructure: ferritic, austenitic and duplex

[6,9]. Melting and alloying is the first step in making any steel, this can be especially difficult when dealing with high contents of reactive alloying elements. The solidification steels is the next important step in the production rout, not only dictating the casting method (continuous or ingot), it also has great influence on the microstructure and further processing. Hot working is the third important step, as it restricts the shape and initial microstructure before the heat treatment. Finally the heat treatment rounds up the mechanical properties and microstructure. The present study aims to clarify the microstructural evolution during the production of low-density multiphase steels, few cases are presented to show the complexity of the process. Ferrite-austenite duplex low-density Fe-15Mn-10Al-0.8C (wt%) steel was produced and remelted to analyse the temperatures and volume fractions of solidification phases, the results were compared with thermodynamic calculations. 5 %Ni additions were made according to the results of Kim et al. and Rahnama et al [10,11]. The Ni addition changes the precipitations phases and their chemical compositions that affect the mechanical properties [11].

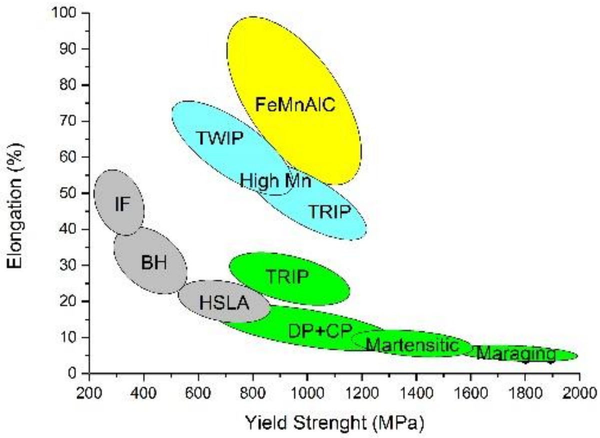

Figure 1 Steel strength ductility “Banana” diagram for commercial and emerging steel grades

2. EXPERIMENTAL

10 kg steel samples were made in a vacuum induction melting furnace under a protective atmosphere of 300 mbar argon. Pure elements, Al, Mn, Ni, C and mild steel were used to produce the laboratory steel grades. The steel was cast into a 210 mm long ingot that was 80 mm wide at the bottom and 90 mm wide at the top. The cast ingots were homogenised for 2 h at 1200 °C. The samples for DSC were taken from as cast samples. The chemical composition (**Table 1**) was measured by wet chemical analysis and infrared absorption after combustion with ELTRA CS-800. The chemical composition (table 1) was measured by wet chemical analysis and infrared absorption after combustion ELTRACS-800. Two different compositions were made, containing different amounts of Ni.

The samples for optical microscopy were grinded, polished and etched with 8% nital. Samples for scanning electron microscopy electron backscatter diffraction SEM EBSD analysis were grinded and polished by OPS. Metallographic analysis was done with Nikon Microphot FXA optical microscope with Hitachi HV-C20A 3CCD video camera. A JEOL JSM 6500-F scanning electron microscope, equipped with an Oxford energy-dispersive X-ray spectroscopy (EDS) system and Nordlys II EBSD detector was used for SEM analysis. Post processing of the EBSD data was performed in Channel 5 software.Hardness was measured by Vickers method (Instron Tukon 2100B). Differential scanning calorimetry was made in NETZSCH STA 449 C Jupiter thermal analyser. Samples were heated up to 1550 °C at 10 K/min in protective Ar atmosphere, cooling was also carried out at 10 K/min to room temperature. Since we were investigating solidification of the low-density steel, we used just cooling curves for further analysis. We used commercial software Thermo-Calc 2020b, database TCFE10 for CALPHAD modelling. We used Equilibrium Calculator, namely, the Property Diagram to obtain phase diagrams.

3. RESULTS AND DISSCUSSION

The melting in the VIM was done at 300 mbar Ar atmosphere due to the high evaporation rate of Mn and partially Al under higher vacuum. The two different chemical compositions are given in **Table 1**.

Table 1 Chemical analysis of the investigated steels (mass%)

Sample	C	Si	Mn	Ni	Al	Fe
FeMnAlC	0.83	0.2	15.0	0.1	10.2	Bal.
FeMnAl5.6NiC	0.81	0.20	14.8	5.6	10.1	Bal.

The heating of the charged material and the melt along with vapor pressure of Mn and Al at the processing temperatures are shown in **Figure 2**.

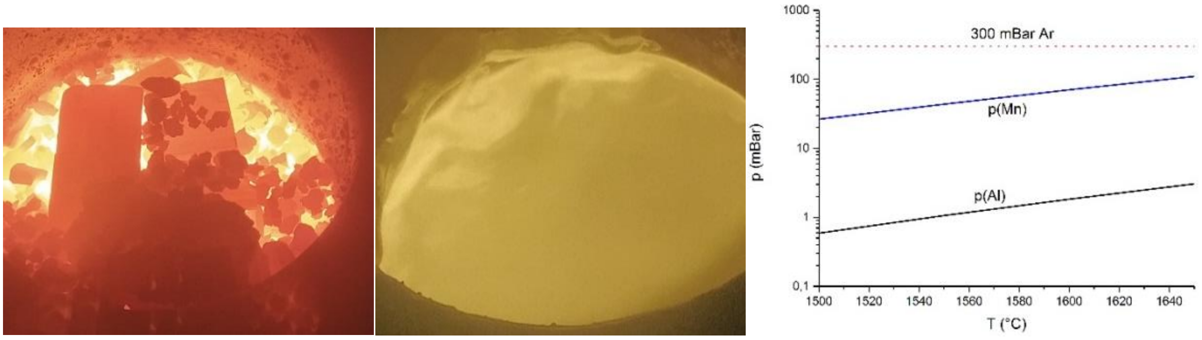

Figure 2 Heating and melting of the charge material and vapour pressure of Mn and Al at processing temperatures

As cast microstructure consists from two phases: δ-ferrite and γ-austenite [12]. The microstructure of FeMnAl5.6NiC is shown where the lighter phase is δ-ferrite and the darker is γ-austenite (**Figure 3**). The dendritic morphology of ferrite shows a typical dendritic microstructure. SEM EBSD analysis revealed, that δ-ferrite contains about 12.2% Al, 11.5% Mn, 7.2% Ni, while γ-austenite contains 9.1% Al, 15.3% Mn and 4.5% Ni.

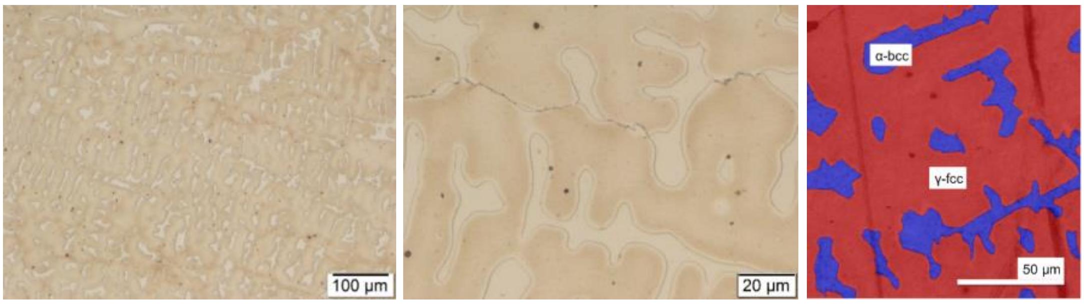

Figure 3 As cast microstructure of FeMnAl5.6NiC

Table 2 Characteristic temperatures (°C) of the investigated steel samples, determined by DSC analysis

Sample	Liquidus	Solidus	Austenite
FeMnAlC	1404	1300	1309
FeMnAl5.6NiC	1375	1266	1286

DSC analysis of the different charges showed that the Ni additions only slightly lowered the liquidus and solidus temperatures, as shown in **Table 2.** The DSC cooling curves of the investigated steels are presented in

Figure 4, the two peaks that occur during solidification are visible on all the DSC curves. In fact, no other transformations were detected. First peak belongs to the solidification of δ-ferrite and second one to the solidification of γ-austenite [13].

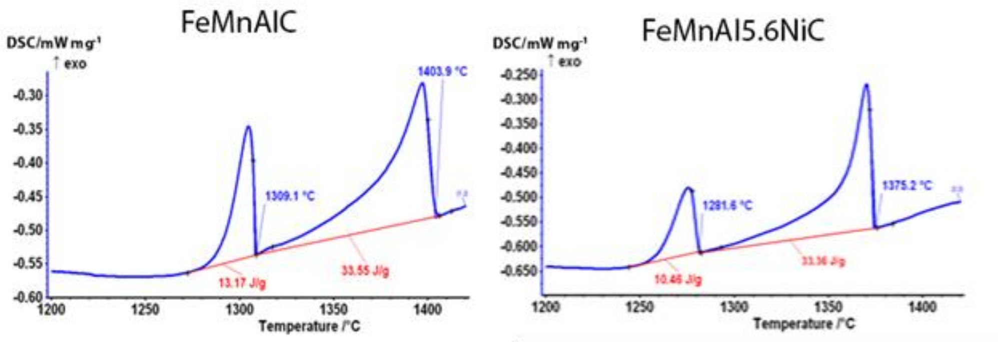

Figure 4 DSC cooling curves for FeMnAlC and FeMnAl5.6NiC

The samples were hot forged at 1200 °C, some edge cracking occurred and the microstructural analysis showed a different microstructure from the as cast one, mainly the transformation of the austenite phase and precipitation along the grain boundaries, the edge cracks occurred both along ferrite and on the ferrite/austenite grain boundaries, as shown in **Figure 5**.

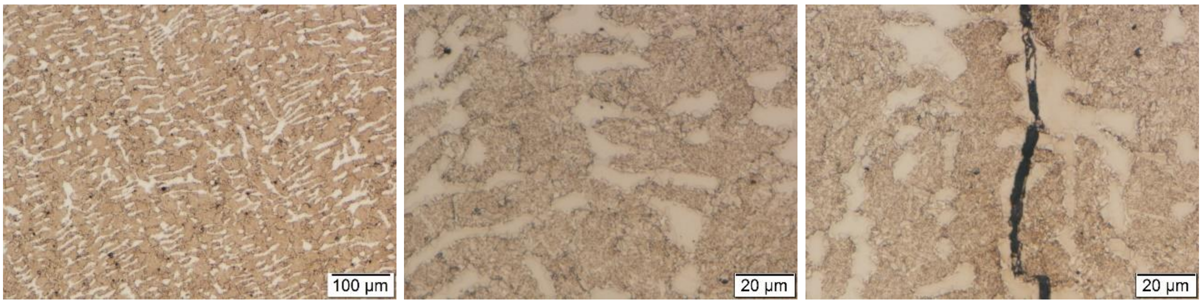

Figure 5 Hot forged microstructure of FeMnAl5.6NiC

The Calphad modelling revealed the formation of Kappa carbides and ordered B2 phase below 1200 °C as shown in **Figure 6**.

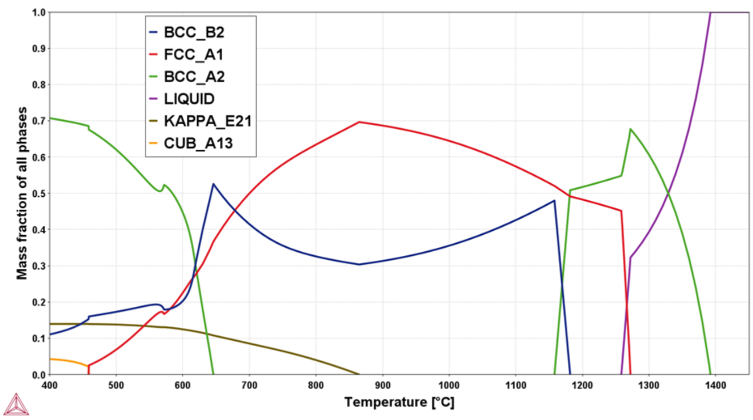

Figure 6 Equilibrium phase composition at different temperatures for sample FeMnAl5.6NiC

The samples were solution annealed at different temperatures, samples that were solution annealed at 1200 °C for 1 h and water quenched showed a two phase microstructure, while samples that were annealed at lower temperatures (1100 and 1000 °C) still had precipitates, slower cooling medium such as air and insulation wool also resulted in partial austenite decomposition (shown in **Figure 7**).

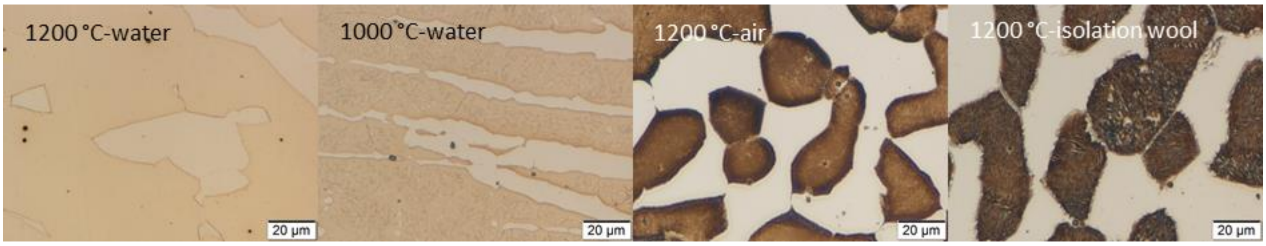

Figure 7 Annealed microstructures of FeMnAl5.6NiC

After the solution annealing at 1200 °C followed by water quenching, the samples were annealed at different temperatures to investigate the effects of precipitation hardening. The samples were annealed for 2h at 300, 400, 500, 600, 700, 800 and 900 °C. The hardness of the samples with higher Ni were higher, the hardness grew to 700 °C and then fell in the FeMnAlC samples, but the maximum was reached at 800 °C for the FeMnAl5.6NiC steel, as seen in **Figure 8**. **Figure 9** shows FeMnAl5.6NiC after annealing at 600 °C.

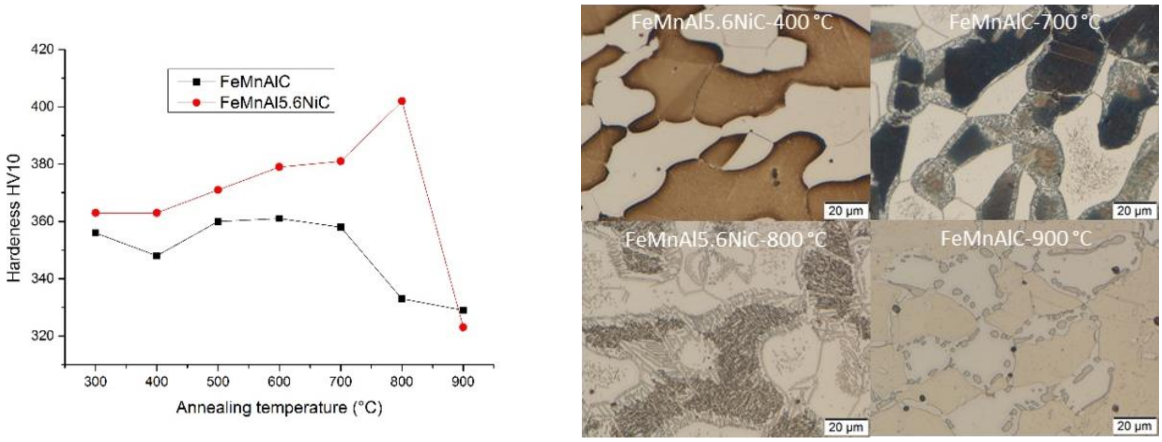

Figure 8 Hardness and some microstructures of solution annealed and precipitation annealed samples of FeMnAlC and FeMnAl5.6NiC

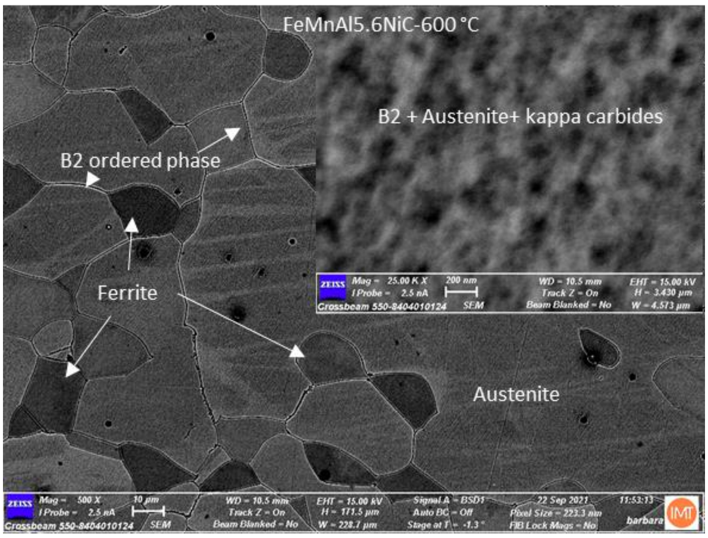

Figure 9 SEM analysis of FeMnAl5.6NiC sample solution annealed sample that was precipitation hardened at 600 °C

The microstructural analysis revealed that the precipitation of kappa carbides and B2 ordered phase were the reason for precipitation hardening during annealing. While the precipitation is mild at lower temperatures (500 °C), it intensifies at 700 °C and in even more intense for FeMnAl5.6NiC at 800 °C, the precipitates begin to coarsen, and their hardening effect is lost at 900 °C, as some even dissolve in the matrix. The precipitation of the B2 ordered phase and kappa carbides was proven b SEM analysis.

4. CONCLUSION

The topic of lightweight FeMnAlC steels is very wide as it offers not only new alloying systems but also very diverse heat treatments. The steels require special care when melting, alloying and hot working. The hardness of well over 300 HV are promising, but further mechanical test are needed to obtain a full spectrum of mechanical properties. The hardness values ranged from 320 to 400 HV, with very different microstructures. The steels are very susceptible to precipitation of different phases and cracking during hot working and cooling. The quenching can prove difficult for internal stresses, especially in larger samples.

REFERENCES

[1] AJANOVIC, A., HAAS, R. The impact of energy policies in scenarios on GHG emission reduction in passenger car mobility in the EU-15. *Renew. Sustain. Energy Rev.* 2017, vol. 68, pp. 1088-1096.

[2] LODI, C., SEITSONEN, A., PAFFUMI, E., DE GENNARO, M., HULD, T., MALFETTANI, S. Reducing CO2 emissions of conventional fuel cars by vehicle photovoltaic roofs. *Transp. Res. Part D Transp. Environ.* 2018, vol. 59, pp. 313-324.

[3] CHEN, S., RANA, R., HALDAR, A., KUMAR, R. Current state of Fe-Mn-Al-C low density steels. *Prog. Mater. Sci.* 2017, vol. *89*, pp. 345-391.

[4] SLATER, C., HOLLYHOKE, N., DAVIS, C. The influence of alloy composition on the as-cast grain structure in near net shape low-density steels. *Ironmak. Steelmak.* 2019, vol. 46, pp. 725-730.

[5] RAABE, D., TASAN, C. C., SPRINGER, H., BAUSCH, M. From high-entropy alloys to high-entropy steels. *Steel Res. Int.* 2015, vol. *86*, pp. 1127-1138.

[6] LEE, J., PARK, S., KIM, H., JUN, S., KEUNHO, P., MI, L., KIM, Y., MADAKASHIRA, P. P., NAM, H. Simulation of κ - Carbide Precipitation Kinetics in Aged Low - Density Fe - Mn - Al - C Steels and Its Effects on Strengthening. *Met. Mater. Int.* 2018, vol. 24, pp. 702-710.

[7] SONG, H., SOHN, S. S. U., KWAK, J., LEE, B., LEE, S. Effect of Austenite Stability on Microstructural Evolution and Tensile Properties in Intercritically Annealed Medium-Mn Lightweight Steels. *Metall. Mater. Trans. A.* Vol. *47*, pp. 2674-2685.

[8] FROMMEYER, G., BRÜX, U. Microstructures and Mechanical Properties of High-Strength Fe-Mn-Al-C Light-Weight TRIPLEX Steels. *Steel Res. Int.* 2006, vol. *77*, pp. 627-633.

[9] KIM, H.; SUH, D. W.; KIM, N. J. Fe-Al-Mn-C lightweight structural alloys: A review on the microstructures and mechanical properties. *Sci. Technol. Adv. Mater.* 2013, vol. 14.

[10] KIM, S., KIM, H., KIM, N. J. Brittle intermetallic compound makes ultrastrong low-density steel with large ductility. *Nature.* 2014, vol. 518, pp. 77-79.

[11] RAHNAMA, A., KOTADIA, H., SRIDHAR, S. Acta Materialia Effect of Ni alloying on the microstructural evolution and mechanical properties of two duplex light-weight steels during different annealing temperatures : Experiment and phase- field simulation. *Acta Mater.* 2017, vol. 132, pp. 627-643.

[12] BURJA, J., BATIČ, B. Š., BALAŠKO, T. Influence of the addition of Ni on as-cast microstructure of duplex Fe-Al-Mn-Ni-C lightweight steel. *Crystals.* 2021, vol. 11.

[13] BALAŠKO, T., BURJA, J., MEDVED, J. Effect of Ni on solidification of duplex low-density steels. *J. Therm. Anal. Calorim.* 2020.